Modeling Magnetotail Ion Distributions with Global Magnetohydrodynamic and Ion Trajectory Calculations

M. El-Alaoui, M. Ashour-Abdalla, J. Raeder, V. Peroomian

Institute of Geophysics and Planetary Physics, University of California, Los Angeles, CA 90095-1567

L. A. Frank, W. R. Paterson

Department of Physics and Astronomy, The University of Iowa, Iowa City

J. M. Bosqued

Centre d'Etude Spatiale des Rayonnements, CNRS, Toulouse, France

On February 9, 1995, the Comprehensive Plasma Instrumentation (CPI) on the Geotail spacecraft observed a complex, structured ion distribution function near the magnetotail midplane at $x \sim -30\ R_E$. On this same day the Wind spacecraft observed a quiet solar wind and an interplanetary magnetic field (IMF) that was northward for more than five hours, and an IMF B_y component with a magnitude comparable to that of the IMF B_z component. In this study, we determined the sources of the ions in this distribution function by following approximately 90,000 ion trajectories backward in time, using the time-dependent electric and magnetic fields obtained from a global MHD simulation. The Wind observations were used as input for the MHD model. The ion distribution function observed by Geotail at 1347 UT was found to consist primarily of particles from the dawn side low latitude boundary layer (LLBL) and from the dusk side LLBL; fewer than 2% of the particles originated in the ionosphere.

1. INTRODUCTION

A fundamental goal of magnetospheric physics has been to determine the mechanism for transport of plasmas through the solar wind-magnetosphere-ionosphere system. Growing evidence indicates that the solar wind and the ionosphere, the main sources of hot plasma in the magnetosphere, contribute roughly comparable amounts [*Shelley et al.*, 1982; *Lennartsson and Shelley*, 1986]. The most definitive information on relative contributions of the ionosphere and the solar wind has been deduced from ion composition measurements, with O^+ ions used as tracers of ionospheric plasma and He^{++} ions used as solar wind tracer ions. The H^+ ions that make up a large fraction of the plasma, however, may come from either source. This study focuses only on H^+.

To understand the transport of plasma through the solar wind-magnetosphere-ionosphere system, it is necessary to determine not only the sources of the plasma, but

Geospace Mass and Energy Flow: Results From the International Solar-Terrestrial Physics Program
Geophysical Monograph 104

also its transport mechanisms throughout the magnetosphere and the geomagnetic tail. The MHD models yield a picture of the overall configuration of the magnetosphere and bulk transport, but the MHD paradigm neglects important physics such as particle drift motion. To address this deficiency, we used time-dependent Large-Scale Kinetics (LSK) to determine the history of the particles in the measured distribution function and then used this information to extend the capability of the MHD model. In this paper we apply an approach in which we use both numerical simulations and observations to study the origins and transport of magnetotail plasma. We begin with a global magnetohydrodynamic (MHD) simulation of the interaction between the solar wind and the magnetosphere that employs observed solar wind and interplanetary magnetic field (IMF) parameters for the solar wind boundary conditions of the simulation [*Ashour-Abdalla et al.*, this issue]. The MHD code is run to model the time dependent response of the magnetosphere to the changing solar wind and to obtain the global magnetic and electric fields [*Raeder et al.*, 1997]. Next we launch ions in accordance with an observed distribution function and follow the trajectories backwards in time in the MHD electric and magnetic fields [*El-Alaoui et al.*, 1995; *Ashour-Abdalla et al.*, 1997*a*]. We chose to apply this approach first to a study of the "quiet" magnetosphere when the IMF is northward for an extended time. Although the magnetosphere is less dynamic during intervals of northward IMF, the magnetic configuration is still very complex.

2. OBSERVATIONS

On February 9, 1995, between 0800 UT and 1400 UT the Wind spacecraft was located near (190, 40, 2) R_E in GSE coordinates. The observed IMF and the solar wind parameters were quite stable for the entire 6 hours. During this time interval a northward IMF (B_z ~ 5 nT) with a significant B_y component was observed. The B_y component was directed duskward and was comparable in magnitude to the B_z component. The solar wind speed and density averaged roughly 400 km/s and 5 cm^{-3} respectively. During this same time interval the Geotail satellite was located in the tail, 30 R_E from Earth. Plate 1 shows v_y - v_z, v_x - v_z and v_x - v_y cuts of the 3-D ion distribution function measured at 1347 UT by the Hot Plasma Analyzer (HP) of the Comprehensive Plasma Instrumentation (CPI) [*Frank et al.*, 1994]. The arrow (in the middle panel) represents the projection of the magnetic field vector onto the z - x plane. This distribution function is non-Maxwellian and has additional structures in the direction perpendicular to the magnetic field. The distribution is also warmer than in the previous time interval (not shown here) [*Ashour-Abdalla et al.*, 1997*c*].

3. METHODOLOGY

The IMF and solar wind data from the Wind spacecraft were used as input to a global MHD simulation. The simulation was validated by comparing its magnetic field and flow velocity time series at the nominal Geotail location (30 R_E downtail) with those observed by Geotail from the time interval 0800 UT to 1400 UT (see *Ashour-Abdalla et al.* [1997*c*] for a complete description). The comparison showed reasonable agreement between the model's results and the observations for the period when Geotail was in the boundary of the plasma sheet. However, the MHD simulation did not reproduce the multiple penetrations of the central plasma sheet made by the Geotail spacecraft, though the agreement was better when the "virtual satellite" in the MHD model was moved upward in z by 1.5 R_E. This lack of agreement was evidently a result of the fact that Geotail was in a region of steeper gradients than those reproducible within the spatial resolution of the MHD model.

The 3-D distribution function shown in Plate 1 was partitioned into (75 km/s)^3 bins with the number of model ions in each v_x - v_y - v_z bin chosen to be proportional to the phase space density measured by Geotail for each bin. The fine-scale structure of the observed distribution was preserved in this partitioned distribution function. We followed the trajectories of 90,000 noninteracting ions in the time dependent MHD electric and magnetic fields backward in time until they reached their origin, i.e. the magnetopause (as determined from the MHD total current) or the ionosphere (taken to be those particles approaching to within 3.7 R_E of the Earth). Magnetic and electric fields were obtained from the global MHD calculations at four minute intervals. We used linear interpolation in space and time to obtain the field values between time and spatial grid points for the trajectory calculations. In these calculations the electric field was taken to be

$$\vec{\mathbf{E}} = -\vec{\mathbf{U}} \times \vec{\mathbf{B}} + \eta\vec{\mathbf{J}}$$

where $\vec{\mathbf{U}}$ is the bulk flow velocity, $\vec{\mathbf{B}}$ is the magnetic field, $\vec{\mathbf{J}}$ is the current density, and η is the resistivity. Resistive ($\eta\vec{\mathbf{J}}$) contributions to $\vec{\mathbf{E}}$ become significant only near the magnetopause and near the x-lines. A 4th order Runge-Kutta method was used to integrate the ion trajectories with respect to time. One time step in the

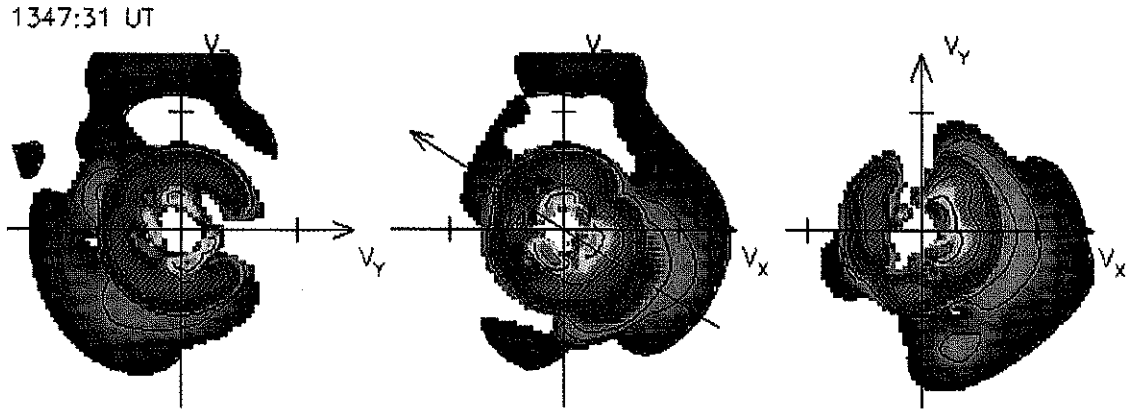

Plate 1. Velocity distribution function measured by Geotail on February 9, 1995, at 1347 UT.

particle trajectory calculation was 0.002 of the local ion gyro-period, with an upper limit applied to prevent the time step's becoming too large in weak field regions.

4. RESULTS

The calculated points of origin for all of the simulation's ions are shown in Plate 2. The upper left panel shows these points projected onto the noon-midnight meridian plane ($y = 0$), and in the lower left panel they are projected onto the equatorial plane ($z = 0$). Solid black curves indicate the intersections of the magnetopause with the $y = 0$ and $z = 0$ planes. The color scale to the right of each panel denotes the number of particles in each 1 $R_E \times 1$ R_E bin. The particles come from both the dawn and the dusk flanks of the magnetosphere, and the sources form broad bands in the y and z directions along the magnetopause.

For the dusk side magnetopause, the upper left panel shows that the source region is localized around $z = 0$ at $x = -30$ R_E. Further downtail, the particles enter at larger values of z, reaching as high as the vicinity of $z = 10$ R_E at $x = -120$ R_E. Most of the particles from the dusk side magnetopause come from 0 to 30 R_E down the tail. Further down the tail the density of the entering particles is very low, with only a few particles per bin. The dawn side magnetopause particle entry is concentrated much further downtail. The density of the particles per bin increases downtail on the dawn side magnetopause, with the peak density occurring between -90 R_E and -120 R_E. The entry region is near $z = -10$ R_E at $x = -120$ R_E. The ionospheric contribution (labeled "ionosphere" in Plate 2) is small, providing only 2% of the ions in the observed Geotail distribution. This is because Geotail was relatively far from the Earth (~ 30 R_E). Also, the IMF was steady and northward for more than 6 hours on this day and had a large B_y component. The ionosphere is therefore not a viable source of plasma for this time period. The right panel of Plate 2 shows the MHD current density as a function of y and z at $x = -100$ R_E, and reveals the twisting of the magnetotail. The black dots are projections of all of the ion entry points onto this plane ($x = -100$ R_E). It can be seen that the entry regions correspond to the LLBL. The twisting of the tail explains the location of the LLBL above (below) $z = 0$ on the dusk (dawn) side.

In Plate 3 the v_y - v_z, v_x - v_z and v_x - v_y cuts of the initial 3-D Geotail ion distribution function are color coded according to the source regions of the ions. If more than 75% of the particles in a bin have been supplied by a single source, the bin is given the color indicating that source; otherwise the bin is black. No bin is dominated by the ionospheric source. The low energy particles streaming tailward along the x axis are mainly from the dusk side LLBL (red dots). The particles streaming earthward are from the dawn side LLBL (green dots). The higher energy part of the tailward streaming distribution is also populated by the dawnside LLBL (Plate 3*a*, 3*b*).

Figure 1 and Figure 2 show two typical test particle trajectories from our calculations. The top panel of each figure displays an individual trajectory in a three-dimensional perspective, and the lower panel of each figure shows the particle energy versus time with the parameter of adiabaticity κ (shown with gray dots) superimposed [*Büchner and Zelenyi*, 1986, 1989]. κ is defined as

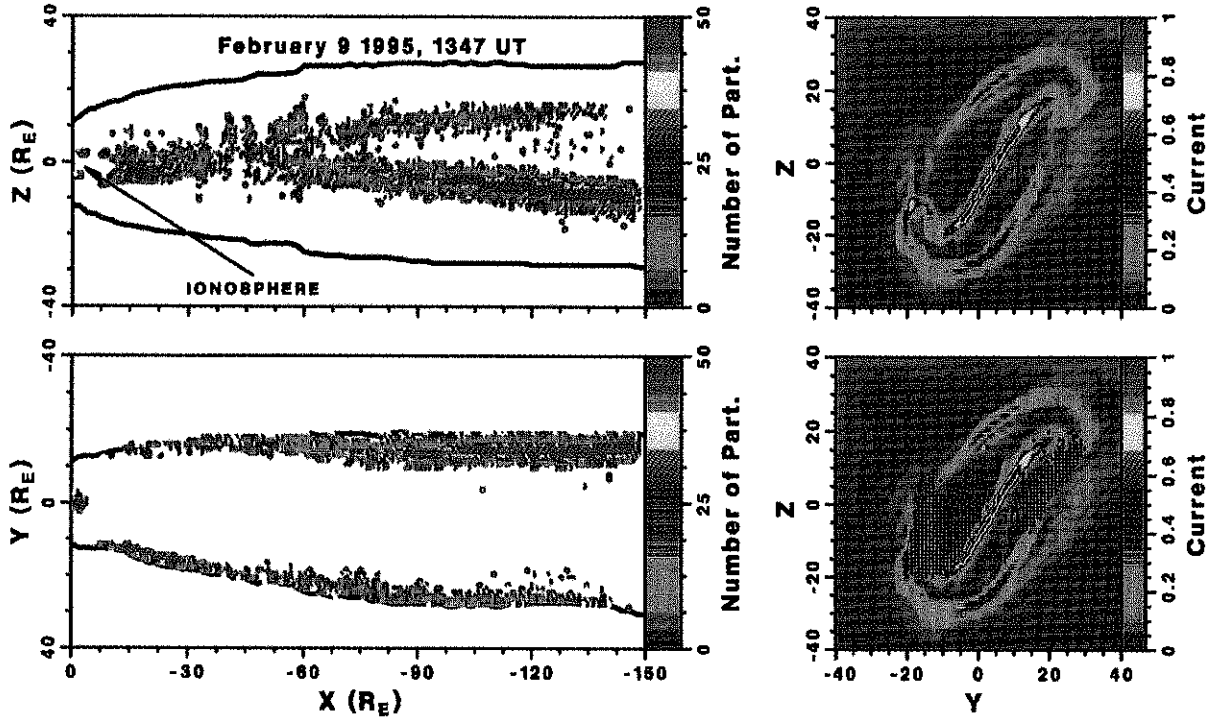

Plate 2. Magnetospheric entry points for all particles projected onto the x-y (lower left-hand panel) and x-z planes (upper left-hand panel). The upper right panel shows a cross section o the MHD total current density at the Geotail location (x = - 30 R_E) at 1347 UT. This panel shows the twisting of the geomagnetic tail around the Sun-Earth axis toward the dusk side. The lower right-hand panel shows a projection of all entry points onto this plane (black dots).

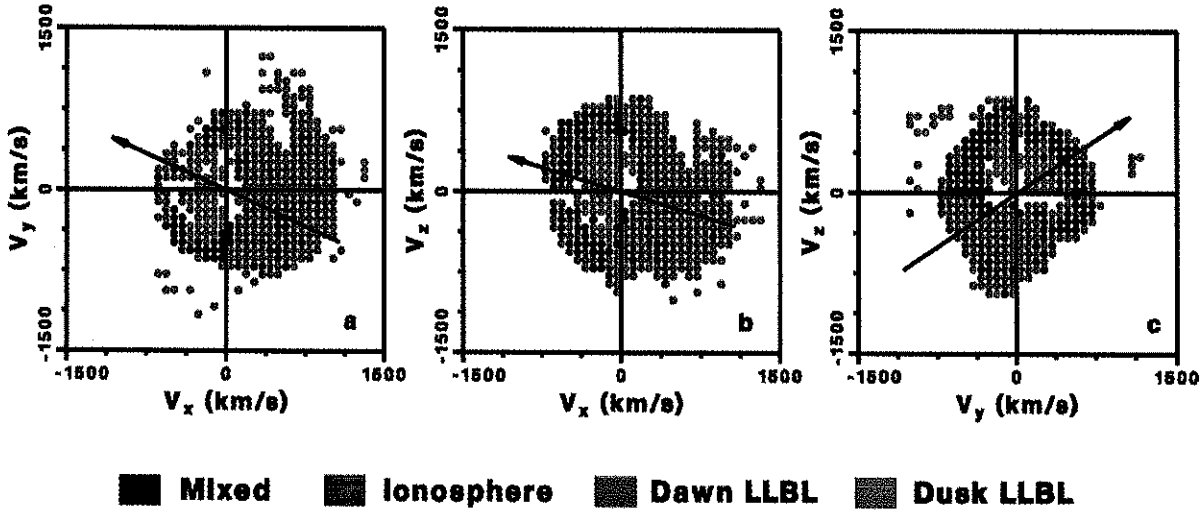

Plate 3. 3-D cuts of the velocity distribution function color-coded according to dominant particle source. The color table is shown below the figure.

$$\kappa \equiv \sqrt{R_c/\rho_L}$$

where R_c is the local magnetic field radius of curvature and ρ_L is the ion Larmor radius. The upper panel of Figure 1*a* depicts an ion that originated in the dawn side magnetopause at $x \sim -90\ R_E$, where it has a kinetic energy of ~ 2 keV. The particle crosses the magnetotail from dawn to dusk, executes several nonadiabatic ($\kappa \leq 1$) interactions with the current sheet (gray dots in the lower panel) during which it gains energy, and finally arrives at Geotail (green dot) with an energy of ~ 4 keV. This type of particle makes up the bulk of the distribution measured in the direction perpendicular to $\vec{\mathbf{B}}$.

Figure 2 shows a particle that enters the magnetosphere at $x \sim -20\ R_E$ on the dusk side of the magnetosphere. This ion becomes trapped on near-Earth closed field lines, the particle then executes several adiabatic ($\kappa >> 1$) bounces while drifting dawnward until it encounters Geotail. This orbit is representative of the ions entering the magnetosphere on the dusk flank between $x = -10\ R_E$ and $-30\ R_E$ (see Plate 2). The particle's energy does not change significantly during its journey and the particle arrives at Geotail (shown by the green dot) with an energy of 2 keV.

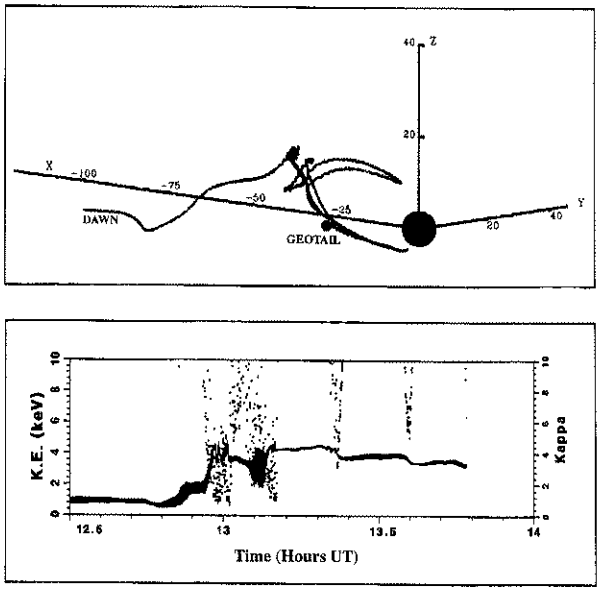

Figure 1. Trajectory of a typical ion from the dawn side LLBL measured by Geotail at 1347 UT. The upper panel shows a three-dimensional perspective of the particle's trajectory. The lower panel shows the particle's kinetic energy (scale on the left), and κ (gray dots, scale on the right).

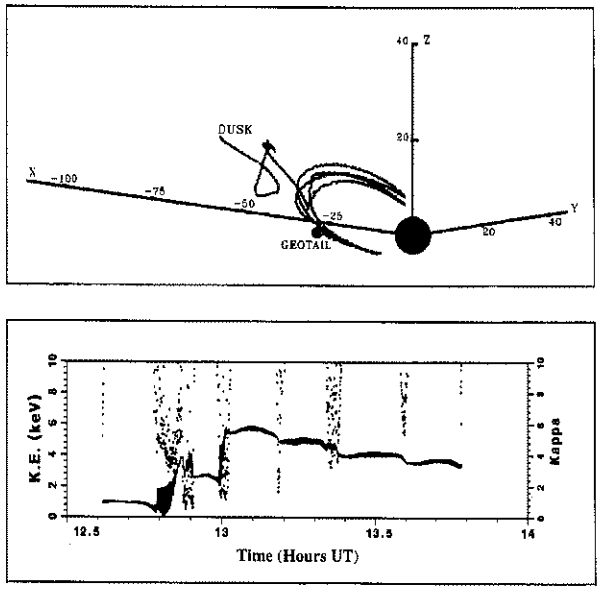

Figure 2. Trajectory of a typical ion from the dusk side LLBL measured by Geotail at 1347 UT. The figure is in the same format as Fig. 1.

5. SUMMARY

The calculations presented in this paper were based on observations made on February 9, 1995, by the Wind spacecraft, positioned upstream of the magnetosphere in the solar wind, and by the Geotail satellite, located 30 R_E downtail, while the IMF was northward and all solar wind parameters were steady. A relatively large B_y component led to a magnetospheric configuration unlike any that had previously been produced by analytical models or idealized simulations. The complexity of the magnetosphere during this time period resulted from the twisting of the tail around the Sun-Earth axis toward the dusk side. Test particles were launched at the Geotail location (-29.,1.53,-2.58) R_E and were followed backward in time through an MHD field model, which was also regressed through its previous states. This time-dependent large scale kinetic study identified the origins of different ion subsets of the ion velocity distribution function measured on February 9, 1995, at 1347 UT by Geotail. The results can be summarized as follows:

1. The IMF B_y component caused a twisting of the magnetotail current sheet. Because the IMF B_y was steady for more than 6 hours, the magnetotail cross section showed little change as a function of time.

2. Two sources, the dawn side LLBL and the dusk side LLBL, contributed most of the observed ion population.

3. The ionospheric contribution was minor, making up only 2% of the ions observed by Geotail. The smallness of this contribution could be a result of the following factors: 1) the IMF was northward for an interval of more than 6 hours; and 2) Geotail was postitioned beyond $x \sim -20\ R_E$, a region where the ionospheric contribution to the magnetotail plasma population may be small [e.g. *Lennartsson and Shelley*, 1986].

4. The dawn side LLBL ions interacted with the current sheet tailward of Geotail. These particles experienced nonadiabatic ($\kappa < 1$) behavior and were substantially energized during their neutral sheet crossing. They accounted for the earthward streaming portion of the distribution function and the outer edge of the tailward streaming portion. The source density of these particles increased downtail.

5. The dusk side LLBL ions reached the Geotail location mainly by convecting adiabatically earthward from the duskward flank of the magnetosphere to form the low energy part of the tailward streaming portion of the distribution function. In contrast to the dawn side entry, the peak in the dusk side entry region occurred earthward of Geotail. The dusk side ions became trapped in adiabatic trajectories as soon as they entered the magnetosphere and arrived at Geotail while streaming tailward.

Acknowledgments. The authors thank K. Ogilvie for providing the Wind plasma data and R. P. Lepping for providing the Wind IMF data. We also thank R. L. Richard for helpful discussions. This work was supported by NASA grants NAG5-1100 and NAGW-4553. Computing support was provided by the Cornell Theory Center, the UCLA Office of Academic Computing, the Maui High Performance Computing Center and the San Diego Supercomputer Center. UCLA/IGPP publication number 4937.

REFERENCES

Ashour-Abdalla, M., et al., Ion sources and acceleration mechanisms inferred from local distribution functions, *Geophys. Res. Lett.*, *24*, 955, 1997*a*.

Ashour-Abdalla, M., et al., Determination of particle sources for a Geotail distribution funcion observed on May 23, 1995, in *Geophysical Monograph Series, Global Observations and Models in the ISTP Era*, edited by J. Horwitz, G. L. Gallagher, and W. K. Peterson, this issue, 1997*b*.

Ashour-Abdalla, M., J. Raeder, M. El-Alaoui, and V. Peroomian, Magnetotail structure and its internal particle dynamics during northward IMF, in *Geophysical Monograph Series, The Earth's Magnetotail: New Perspectives*, edited by A. Nishida, submitted, 1997c.

Büchner, J., and L. M. Zelenyi, Deterministic chaos in the dynamics of charged particles near a magnetic field reversal, *Phys. Lett. A*, *118*, 395, 1986.

Büchner, J., and L. M. Zelenyi, Regular and chaotic charged particle motion in magnetotail-like field reversals, 1. Basic theory of trapped motion, *J. Geophys. Res.*, *94*, 11821, 1989.

El-Alaoui, M., M. Ashour-Abdalla, J. Raeder, and J. M. Bosqued, Simulation of ion trajectories in the magnetotail using time-dependent electromagnetic fields, in AGU Spring Meeting, Baltimore, (*EOS*, vol. 76, no. 16), 1995.

Frank, L. A., K. L. Ackerson, W. R. Paterson, J. A. Lee, M. R. English, and G. L. Pickett, The Comprehensive Plasma Instrumentation (CPI) for the GEOTAIL spacecraft, *J. Geomagn. Geoelec.*, *46*, 23, 1994.

Lennartsson, W., and E. G. Shelley, Survey of 0.1- to 16-keV/e plasma sheet ion composition, *J. Geophys. Res.*, *91*, 3061, 1986.

Raeder, J., J. Berchem, M. Ashour-Abdalla, L. A. Frank, W. R. Paterson, K. L. Ackerson, S. Kokubun, and T. Yamamoto, and J. A. Slavin, Boundary layer formation in the magnetotail: Geotail observations and comparisons with a global MHD model, *Geophys. Res. Lett.*, *24*, 951, 1997.

Shelley, E. G., W. K. Peterson, A. G. Ghielmetti, and J. Geiss, The polar ionosphere as a source of energetic magnetospheric plasma, *Geophys. Res. Lett.*, *9*, 941, 1982.

Mostafa El-Alaoui, Maha Ashour-Abdalla, Joachim Raeder , and Vahé Peroomian, Institute of Geophysics and Planetary Physics, University of California, Los Angeles, CA 90095-1567 (e-mail mostafa@igpp.ucla.edu).

L. A. Frank, and W. R. Paterson, Department of Physics and Astronomy, The University of Iowa, Iowa City, IA 52242.

J. M. Bosqued, Centre d'Etude Spatiale des Rayonnements, CNRS, BP 4346, 31029 Toulouse Cedex, France.